Dynamics of mitochondrial Ca^{2+} uptake in MICU1-knockdown cells

Sergio de la Fuente, Jessica Matesanz-Isabel, Rosalba I Fonteriz, Mayte Montero and Javier Alvarez[1]

Instituto de Biología y Genética Molecular (IBGM), Departamento de Bioquímica y Biología Molecular y Fisiología, Facultad de Medicina, Universidad de Valladolid and Consejo Superior de Investigaciones Científicas (CSIC), Ramón y Cajal, 7, E-47005 Valladolid, SPAIN.

[1]To whom correspondence should be addressed: phone: +34-983184844, fax: +34-983423588, e-mail: jalvarez@ibgm.uva.es

Abstract

MICU1 is an important regulator of the mitochondrial Ca^{2+}-uniporter (MCU) that has been recently shown to act as a gatekeeper of MCU at low cytosolic $[Ca^{2+}]$ ($[Ca^{2+}]_c$). We have studied here in detail the dynamics of MCU activity after shRNA-knockdown of MICU1 and we find several new interesting properties. In MICU1-knockdown cells, the rate of mitochondrial Ca^{2+}-uptake was largely increased at low $[Ca^{2+}]_c$ (<2μM), but it was decreased at high $[Ca^{2+}]_c$ (>4μM). In the 2-4μM range, a mixed behavior was observed, where mitochondrial Ca^{2+}-uptake started earlier in the MICU1-silenced cells but slower than in the controls. Sensitivity of Ca^{2+}-uptake to ruthenium red and Ru360 was similar at both high and low $[Ca^{2+}]_c$, indicating that the same Ca^{2+}-pathway was operating in both cases. The increased Ca^{2+}-uptake rate observed at $[Ca^{2+}]_c$ below 2μM was transient and became inhibited during Ca^{2+}-entry. Development of this inhibition was slow, required 5 min for completion, and was hardly reversible. Therefore, MICU1 acts both as a MCU gatekeeper at low $[Ca^{2+}]_c$ and as a cofactor necessary to reach the maximum Ca^{2+}-uptake rate at high $[Ca^{2+}]_c$. Moreover, in the absence of MICU1, MCU becomes sensitive to a slow-developing inhibition that requires prolonged increases in $[Ca^{2+}]_c$ in the low micromolar range.

Summary

MICU1 functions as MCU gatekeeper at low $[Ca^{2+}]_c$ (<2μM) and as activator of mitochondrial Ca^{2+}-uptake at high $[Ca^{2+}]_c$ (>4μM), with mixed behavior in the 2-4μM range. Moreover, in MICU1-knockdown cells, MCU undergoes a Ca^{2+}-dependent slow-developing inhibition that restores low MCU-permeability.

Short title: $[Ca^{2+}]_M$ dynamics in MICU1-knockdown cells

Keywords: MCU, MICU1, knockdown, aequorin, mitochondria, Ca^{2+}-uniporter

Abbreviations: $[Ca^{2+}]_M$, mitochondrial $[Ca^{2+}]$; $[Ca^{2+}]_c$, cytosolic $[Ca^{2+}]$; MCU, mitochondrial calcium uniporter. FCCP, carbonyl cyanide 4-trifluoromethoxy)phenylhydrazone.

INTRODUCTION

In recent years, a number of new proteins involved in mitochondrial Ca^{2+} transport have been discovered [1]. MICU1 (mitochondrial calcium uptake 1) was the first one known to be involved in the mitochondrial Ca^{2+} uniporter complex [2]. This complex, the main responsible for Ca^{2+} entry into mitochondria, is now integrated also by the MCU protein, which appears to be the main constituent of the pore across the inner mitochondrial membrane [3-5], and by other regulatory proteins such as MCUR1 [6] and MICU2 [7]. Therefore, as could be expected, mitochondrial Ca^{2+} uptake appears to be a highly regulated process.

The role of MICU1 in the regulation of the mitochondrial Ca^{2+} uniporter is still confuse. It was in fact discovered in a search for mitochondrial proteins whose knockdown in HeLa cells largely reduced mitochondrial Ca^{2+} uptake [2], and that was the proof that it was an essential component of the Ca^{2+} uptake machinery. Given that its predicted structure included only a single membrane-spanning region, it was proposed that it was not the pore, but a regulatory protein essential for the transport. However, it has been recently reported that MICU1 is in fact a gatekeeper that limits MCU-mediated Ca^{2+} influx in order to prevent $[Ca^{2+}]_M$ overload [8]. According to this, the main effect of the absence of MICU1 would be to reduce the Ca^{2+} threshold for the activation of mitochondrial Ca^{2+} uptake, and would have little effects on the kinetic properties of MCU-mediated Ca^{2+} uptake. This view is still under debate, as it has been very recently shown that MICU1 plays also an important role in the cooperative activation of MCU at high cytosolic $[Ca^{2+}]$ [9].

We have studied here in detail the effect of silencing MICU1 on the kinetics of mitochondrial Ca^{2+} uptake in HeLa cells. Our results confirm that the absence of MICU1 largely activates mitochondrial Ca^{2+} uptake at low cytosolic $[Ca^{2+}]$, but show also that the absence of MICU1 reduces Ca^{2+} uptake at higher $[Ca^{2+}]_c$. In addition, we show that the absence of MICU1 reveals a new mode of functioning of the uniporter at low cytosolic $[Ca^{2+}]$, where the increased Ca^{2+} entry induced by MICU1 knockdown undergoes a slow inactivation in the presence of $[Ca^{2+}]_c$ maintained above 200nM.

EXPERIMENTAL

Cell culture, MICU1 knockdown and aequorin expression

HeLa cells stocks are kept frozen in liquid nitrogen. A new stock is opened for use every 2-3 months, and as soon as possible several new samples are frozen again to keep the stock of frozen cells with the minimum passage number. **With this procedure, we calculate that our HeLa cells should have no more than 6-8 extra passages since we originally obtained them.** Both the morphological and functional characteristics of the cells in terms of Ca^{2+} signaling have not significantly changed with time. HeLa cells were grown in Dulbecco's modified Eagle's medium supplemented with 5% fetal calf serum, 100 i.u. ml^{-1} penicillin and 100 i.u. ml^{-1} streptomycin. The constructs for mitochondrially targeted mutated aequorin (Asp119→Ala) and double mutated aequorin (Asp119→Ala and Asn28→Leu) have been described before [10,11]. Human shRNA constructs made to silence the CBARA1 gene (MICU1), were obtained from Origene, Rockville, USA (ref. TF314182). The most effective was ref. TF314182C (TGCAGAATCTCCACCATGTGTAGACAACC), which was used for most of the studies. Constructs include also the red fluorescent protein gene to control expression, and were used both for transient transfections and to make stable silenced clones using puromycin, by following the instructions of the provider. Transfections were carried out using Metafectene (Biontex, Munich, Germany). Preparation of a MCU-silenced HeLa cell clone was described before [11].

The experiments shown in this paper were performed after 48-72h of transfection of this shRNA in HeLa cells (shRNA cells), and compared with controls transfected in parallel with a

scrambled shRNA (scRNA cells). In addition, HeLa cell clones expressing either the MICU1-specific shRNA or the scrambled one were also obtained and used in some experiments. To measure $[Ca^{2+}]_M$ in the case of transient transfections, the plasmids containing either mutated aequorin or double mutated aequorin were cotransfected with the shRNA construct, and cells cotransfected with a scrambled shRNA were used as a control. Measurements were carried out 48-72h after transfection. In the case of the stable silenced clone, cells were transfected with the corresponding mitochondrial aequorin construct, and a stable clone expressing a scrambled shRNA casette was used as a control.

Stable clones were also used to measure the degree of MICU1 knockdown by western blot, using the polyclonal antibody anti-CBARA1 (Abnova) to recognize MICU1 in the cell extracts. Protein extracts were made from stable clones using Radio Immunoprecipitation Assay (RIPA) buffer for cell lysis. Proteins were separated in 12% SDS-PAGE (Bio-Rad), transferred onto polyvinylidene difluoride (PVDF) membranes and tested with the polyclonal antibody anti-CBARA1 (Abnova; dilution 1/500). Monoclonal Anti-actin antibody (BD sciences; dilution 1:10000) was used as the loading control, and was added in a separate lane to avoid overlap with the MICU1 band. Isotype matched, horseradish-peroxidase-conjugated (Amersham; dilution 1:10000) was used as secondary antibody, followed by detection by chemiluminescence (Bio-Rad). The degree of knockdown in transient transfections is more difficult to estimate due to uncertainties in the percentage of transfection. The pattern of dynamic $[Ca^{2+}]_M$ data obtained in the MICU1-knockdown cell clones was similar to that found in the transient transfections. However, the magnitude of the changes in the $[Ca^{2+}]_M$ dynamics induced by MICU1-knockdown was stronger in transient transfections than in stable cell clones, suggesting that the percentage of silencing in the transiently transfected cells is probably higher. In addition, there was no difference in the functional response obtained after either 48 or 72h of transfection, indicating that turnover of MICU1 is very fast and short-term knockdown of this protein is very efficient.

$[Ca^{2+}]_M$ measurements with aequorin.

HeLa cells were plated onto 13 mm round coverslips prior transfection. For aequorin reconstitution, HeLa cells were incubated for 1-2h at room temperature in standard medium (145mM NaCl, 5mM KCl, 1mM $MgCl_2$, 1mM $CaCl_2$, 10mM glucose, and 10mM HEPES, pH 7.4) with 1µM native coelenterazine (for both mutated aequorin and double mutated aequorin, see [11]). Most of the experiments were made using mutated aequorin, except those measuring very high $[Ca^{2+}]_M$ that required using the double mutated one. After reconstitution, cells were placed in the perfusion chamber of a purpose-built luminometer. Then, for experiments in intact cells, cells were perfused with standard medium containing 1mM $[Ca^{2+}]$ followed by the stimuli. For experiments with permeabilized cells, standard medium containing 0.5mM EGTA instead of Ca^{2+} was perfused for 1 min, followed by 1 min of intracellular medium (130mM KCl, 10mM NaCl, 1mM $MgCl_2$, 1mM potassium phosphate, 0.5mM EGTA, 1mM ATP, 20µM ADP, 5mM L-malate, 5mM glutamate, 5mM succinate, 20mM Hepes, pH 7) containing 100µM digitonin. Then, intracellular medium without digitonin was perfused for 5 min, followed by solutions of known $[Ca^{2+}]$ obtained using either EGTA/Ca^{2+} or HEDTA/Ca^{2+}/Mg^{2+} mixtures. Temperature was set at 37ºC. Calibration of the luminescence data into $[Ca^{2+}]$ was made using an algorithm adjusted to the calibration of each aequorin form, as previously described [12,13]. Statistics were made using the ANOVA test.

Measurements of mitochondrial membrane potential.

Mitochondrial membrane potential was monitored using the fluorescent indicator tetramethylrhodamine ethyl ester (TMRE). HeLa cells were placed in a cell chamber in the stage of a Zeiss Axiovert 200 microscope under continuous perfusion, permeabilized as described above and then perfused with intracellular medium containing 20nM TMRE until a steady-state fluorescence was reached (usually about 5 min). Single cell fluorescence was excited at 540 nm using a Cairn monochromator and images of the fluorescence emitted between 570 and 630 nm obtained with a 40x Fluar objective were recorded by a Roper

CoolSnap fx camera. Single cell fluorescence records were analyzed off-line using the Imaging Workbench 6.0 program. Experiments were performed at 37ºC using an on-line heater from Harvard Apparatus.

Materials

Native coelenterazine was obtained from Biotium Inc., Hayward, Ca, U.S.A. Other reagents were from Sigma, Madrid, Spain or Merck, Darmstadt, Germany.

RESULTS

Silencing of MICU1 has been described to increase mitochondrial Ca^{2+} uptake at low [Ca^{2+}] [8]. Instead, Ca^{2+} uptake was either unmodified [8] or decreased [2,9] when high [Ca^{2+}] was present in the cytosolic side of MICU1-depleted mitochondria. We have used here targeted aequorin to study in detail the effect of MICU1 knockdown on mitochondrial Ca^{2+} uptake, and we find several new surprising features on the role of this protein in mitochondrial Ca^{2+} uniporter activation.

Fig. 1 shows the effect of MICU1 knockdown on the $[Ca^{2+}]_M$ peak induced by histamine. When the maximum concentration of histamine was used (panel a), MICU1 knockdown significantly reduced the mitochondrial [Ca^{2+}] peak with respect to that obtained in cells transfected with the scrambled shRNA (scRNA cells) (see the statistics in Fig. 1, panel e). The same happened at 5µM histamine (panel b). However, when cells were stimulated with only 2µM histamine, the $[Ca^{2+}]_M$ peak had the same amplitude in MICU1-knockdown cells (shRNA cells) and in the controls, and the increase in $[Ca^{2+}]_M$ started earlier in the shRNA cells (panel c). Finally, when 0,5µM histamine was used, a much higher $[Ca^{2+}]_M$ increase was obtained in the shRNA cells than in the scRNA ones (panel d). Therefore, MICU1 silencing promotes an earlier activation with increased rate of mitochondrial Ca^{2+} uptake after low-intensity stimuli, while the contrary occurs in the presence of high-intensity stimuli. Panel e shows the statistics of the height of the Ca^{2+} peaks induced by each histamine concentration, and panel f shows the degree of silencing (about 50%) obtained in a cell clone expressing the same shRNA compared with a cell clone expressing a scrambled shRNA. As mentioned in Methods, the degree of silencing is probably higher in transient transfections.

Regarding the resting $[Ca^{2+}]_M$ in MICU1-silenced cells, it has been reported that it becomes significantly increased [8], but other authors found it remains unaltered [2,9]. In our case, we did not find significant differences. The resting $[Ca^{2+}]_M$ in the scramble cells was 128±9nM (mean±s.e., n=7), and in the silenced cells was 127±12nM (mean±s.e., n=7).

We have then used permeabilized cells to study the mitochondrial Ca^{2+} uptake process in more detail. Fig. 2 shows the effect of MICU1 knockdown on mitochondrial Ca^{2+} uptake induced by perfusion of a series of different [Ca^{2+}] buffers in permeabilized cells. After permeabilization, cells were initially perfused with 0,5mM-EGTA-containing medium to ensure that the [Ca^{2+}] is below 10nM. Then, perfusion of 100nM [Ca^{2+}] induced an increase in $[Ca^{2+}]_M$ in shRNA cells (panel a), but no effect in the scRNA ones. In this case, $[Ca^{2+}]_M$ reached a new higher steady-state in the silenced cells and remained stable there. When 200nM [Ca^{2+}] was perfused (panel b), there was again an increase in $[Ca^{2+}]_M$ in the shRNA cells, and a very small response in the scRNA ones. In this case, the increase in $[Ca^{2+}]_M$ in the silenced cells showed an transient overshoot and then decreased to reach a new steady-state. Perfusion of 500nM [Ca^{2+}] (panel c) induced again only a very small increase in $[Ca^{2+}]_M$ in the scRNA cells, and a much larger increase in the shRNA ones. In this case, the overshoot was also much larger, reaching more than twice the final steady-state concentration. Panel d shows the effect of perfusion of 1.5µM [Ca^{2+}] buffer. This concentration was able to trigger a slow but persistent increase in $[Ca^{2+}]_M$ in the scRNA cells, and a very fast but transient increase in the shRNA ones.

When the $[Ca^{2+}]$ in the perfusion buffer was 2.5μM (panel e), the initial increase in $[Ca^{2+}]_M$ was still much faster in the shRNA cells, but the increase stopped soon. Instead, scRNA cells started increasing $[Ca^{2+}]_M$ with a significant delay but they reached a higher final value of $[Ca^{2+}]_M$. Fig. 2e includes also a trace showing the $[Ca^{2+}]_M$ increase induced in scRNA cells by 2μM $[Ca^{2+}]$. This $[Ca^{2+}]$ evokes an increase of $[Ca^{2+}]_M$ in scRNA cells of similar magnitude to that induced by 1.5 μM $[Ca^{2+}]$ in shRNA cells, but without the Ca^{2+}-dependent inhibition, suggesting that this effect actually requires MICU1 silencing. Similar findings were obtained at higher $[Ca^{2+}]$ values in the perfusion buffer. At 3.5μM $[Ca^{2+}]$ (panel f), it is still quite evident that $[Ca^{2+}]_M$ increases much earlier in the shRNA cells. However, scRNA cells start later but increase $[Ca^{2+}]_M$ at a higher rate and rapidly go above the levels reached in shRNA cells. At 4.5 and 10μM $[Ca^{2+}]$, finally, we can only observe that the rate of increase in $[Ca^{2+}]_M$ is larger in the scRNA cells compared with that obtained in shRNA cells (panels g and h).

Fig. 3, panel a, shows the dependence of the $[Ca^{2+}]_M$ increase rate with the extramitochondrial $[Ca^{2+}]$ for both scRNA and shRNA cells, obtained from the data of Fig. 2. The graph shows clearly that silencing of MICU1 increases the rate of mitochondrial Ca^{2+} uptake only at extramitochondrial $[Ca^{2+}]$ below 2.5μM. Instead, for higher extramitochondrial $[Ca^{2+}]$, silencing of MICU1 reduces the rate of $[Ca^{2+}]_M$ uptake. Panel b of this figure shows that MICU1 silenced cells responded faster to the Ca^{2+} addition. The delays shown are the times going from the opening of the perfusion electrovalve to the start of $[Ca^{2+}]_M$ increase, and correspond mainly to the time required for the Ca^{2+} buffer solution to reach the cell coverslip. However, although the same perfusion pathway and electrovalve was used in all the cases, the delays were significantly lower in the shRNA cells with respect to the scRNA cells, for $[Ca^{2+}]$ below 2.5μM.

The lack of difference in the resting $[Ca^{2+}]_M$ between the scRNA and shRNA cells may appear contradictory with the significant $[Ca^{2+}]_M$ increase induced by the addition of 100nM $[Ca^{2+}]$ in shRNA cells, but not in scRNA cells, as seen in Fig. 2a. We have therefore studied if this increase actually leads to a new higher steady-state. Fig. 3c shows that this is not the case. After the initial increase, $[Ca^{2+}]_M$ slowly returned to levels close to the resting values.

To explore some possible mechanisms for the Ca^{2+}-dependent inhibition, we have first performed experiments in the absence of ATP. Perfusing medium without ATP should rapidly wash cytosolic ATP and lead to depletion of mitochondrial ATP through ATP/ADP and ATP/Pi exchangers. If the mechanism of the inhibition involves any phosphorylation, it should be inhibited under these conditions. However, Fig. 3d shows that the inhibition persisted unchanged. An alternative possibility would be the involvement of reactive oxygen species in this phenomenon. We have then tested the dynamics of the Ca^{2+}-dependent inactivation in the presence of four different types of antioxidants, both lipid soluble (100μM α-tocopherol and 100μM lipoic acid) and water soluble (1mM ascorbic acid and 5mM N-methyl-cysteine). None of them produced any effect on the inactivation (**see suppl. Fig. 1**), suggesting that generation of ROS is not involved in the mechanism of that effect.

To be sure that the Ca^{2+} uptake we have measured above occurs in mitochondria and takes place through the Ca^{2+} uniporter, we have tested the effect of the protonophore FCCP and the uniporter inhibitor ruthenium red. Fig. 4, panels a and b, shows that FCCP completely abolished mitochondrial Ca^{2+} uptake both in shRNA and scRNA cells, indicating that mitochondrial membrane potential is required for the $[Ca^{2+}]$ increase. In addition, we have investigated the inhibition by ruthenium red and Ru360 of mitochondrial Ca^{2+} uptake induced by both high (10μM) and low (1.5μM) $[Ca^{2+}]$ in the perfusion buffer, to obtain evidence that it occurred through the same pathway. Our results show that both inhibitors fully blocked mitochondrial Ca^{2+} uptake, no matter if it was induced by high (panels c and e) or low (panels d and f) $[Ca^{2+}]$ in the perfusion buffer. Finally, we show in panels g and h that mitochondrial Ca^{2+} uptake under the same conditions disappeared when a cell clone with silenced MCU was used.

Thus, we can conclude that the Ca^{2+} uptake we measure occurs actually in mitochondria and through the MCU at all the tested $[Ca^{2+}]$.

We have next studied the mechanism of the peculiar dynamics of $[Ca^{2+}]_M$ increase obtained in shRNA cells perfused with low $[Ca^{2+}]$. As shown in Fig. 2, addition of Ca^{2+} in this interval induced a transient increase in $[Ca^{2+}]_M$, which then rapidly decreased to reach a much lower final steady state. Instead, in the scRNA cells, only a smooth increase in $[Ca^{2+}]_M$ was observed in all the range of perfused $[Ca^{2+}]$ buffers. This overshoot suggests the presence of a time-dependent inhibition of the Ca^{2+} pathway in the presence of the $[Ca^{2+}]$ buffer. To test this possibility, we have designed a protocol with two consecutive perfusions of Ca^{2+} buffers, the first one with a variable $[Ca^{2+}]$ (from 100nM to 500nM) and the second one 5 min afterwards with 1.5µM $[Ca^{2+}]$. If the first addition leads somehow to an inhibition of Ca^{2+} transport through the uniporter, the overshoot in the second addition should be significantly decreased with respect to that found in a single 1.5µM $[Ca^{2+}]$ addition. That was the case, and the effect was highly dependent on the $[Ca^{2+}]$ in the $[Ca^{2+}]$ buffer perfused in the first place. Fig. **5** shows that, when the $[Ca^{2+}]$ in that buffer was 100nM, there was no effect in the subsequent Ca^{2+} addition. However, when the $[Ca^{2+}]$ in the buffer was 500nM, the overshoot in the subsequent addition of 1.5µM $[Ca^{2+}]$ disappeared. In the case of the 200nM $[Ca^{2+}]$ buffer, the inhibition of the overshoot in the second addition was partial, so that it was still present, but smaller. Therefore, our data suggest that the first $[Ca^{2+}]$ buffer, in the 200-500nM range, somehow induces an inhibition of the uniporter. Considering that the reduction in the second peak induced by previous perfusion of the 500nM $[Ca^{2+}]$ buffer was 100%, the reduction induced by perfusion of 100nM $[Ca^{2+}]$ was 24±12% (mean±s.e., n=3) and that induced by perfusion of 200nM $[Ca^{2+}]$ was 78±3% (mean±s.e., n=3).

To obtain more information on the mechanism of the inhibition, we studied its time dependence. Fig. **6** shows how the inhibition develops progressively when we increase the time of the first Ca^{2+} perfusion. When the 500nM $[Ca^{2+}]$ buffer was perfused for only 15 or 30 s (panels c and d), there was hardly any effect on the subsequent addition of the 500nM $[Ca^{2+}]$ buffer again 5 min later. It produced a $[Ca^{2+}]_M$ overshoot similar to that found when it was perfused with no previous additions. As the time of the first perfusion of 500nM $[Ca^{2+}]$ was increased to 1-2 min (panels b and c), inhibition of the second one progressively developed. The time required for half inhibition was in fact around 2 min (fig 6f), and the inhibition increased progressively up to values of 80-90% inhibition after 5-10 min of exposure to the 500nM $[Ca^{2+}]$ buffer (fig 6f). The bars diagram in panel f shows the time course of the inhibition of the second peak. The long time required for the inhibition suggests that Ca^{2+} has to enter into the mitochondria and there is a time-requiring mechanism there, because inhibition develops well after the peak of the $[Ca^{2+}]_M$ overshoot. In addition, once produced, the inhibition was very long-lasting. In fact, increasing the time interval in EGTA medium between the two 500nM $[Ca^{2+}]$ additions up to 15 min did not modify the response to the second $[Ca^{2+}]$ addition (data not shown). A partial inhibitory effect was also present when a higher $[Ca^{2+}]$ was perfused in the second addition. Panel g shows that the $[Ca^{2+}]_M$ increase induced by a 3.5µM $[Ca^{2+}]$ buffer was reduced by a 35% if a 500nM $[Ca^{2+}]$ buffer had been perfused before. The inhibition in all these cases was not due to mitochondrial depolarization, as measurement of mitochondrial membrane potential with TMRE did not detect any change after perfusion of the 500nM $[Ca^{2+}]$ buffer (panel h).

We have also tested the effect of 5 min perfusion of the 500nM $[Ca^{2+}]$ buffer on a later $[Ca^{2+}]$ addition in scRNA cells. As shown before, the 500nM $[Ca^{2+}]$ buffer produces in these cells only a small increase in $[Ca^{2+}]_M$. Panel i shows that the second perfusion of 500nM $[Ca^{2+}]$ in these cells produced a $[Ca^{2+}]_M$ increase of similar magnitude, although at a slightly smaller rate. If a 3.5µM $[Ca^{2+}]$ buffer was added in the second perfusion, the increase in $[Ca^{2+}]_M$ was here only slightly, but not significantly, smaller than in the controls (panel j). Thus, perfusion of the 500nM $[Ca^{2+}]$ buffer produces little inhibitory effects in the presence of MICU1.

Discussion

Since the recent discovery of the molecular substrate of the mitochondrial Ca^{2+} uniporter, the MCU protein [3,4], a number of other proteins able to modulate Ca^{2+} transport through MCU have been reported, including MICU2 [7], MCUR1 [6] and particularly MICU1 [2], which was in fact discovered before MCU, and was the first protein found related to mitochondrial Ca^{2+} transport. In fact, with few exceptions, MCU and MICU1 are either both present or both absent across all major branches of eukaryotic life [14]. They are also both present in most tissues, although with a variable relationship among them in terms of mRNA expression [7].

MICU1 has a particularly important role in the regulation of Ca^{2+} flux through MCU stimulated by low submicromolar cytosolic $[Ca^{2+}]$. Mallilankaraman et al., [8] found that silencing of MICU1 largely activates mitochondrial Ca^{2+} uptake at low cytosolic $[Ca^{2+}]$, but has no effects at high cytosolic $[Ca^{2+}]$, concluding that it behaves as a gatekeeper of MCU, blocking Ca^{2+} entry into mitochondria during $[Ca^{2+}]_c$ increases of low magnitude. More recently, Csordas et al. [9] found that MICU1 not only controls the threshold for activation of MCU by $[Ca^{2+}]_c$, but it also plays an important role in the cooperative activation of MCU by higher levels of $[Ca^{2+}]_c$, so that in the absence of MICU1 the rate of Ca^{2+} uptake by mitochondria at high $[Ca^{2+}]_c$ is significantly lower. Our data here confirm this double role of MICU1, both as a gatekeeper of MCU at low submicromolar $[Ca^{2+}]_c$ and as an activator of Ca^{2+} uptake at high $[Ca^{2+}]_c$, and we use the ability of aequorin to explore different $[Ca^{2+}]$ ranges to study the mechanism of these effects in more detail. In addition, our data reveal several novel surprising details on the mechanism of regulation of MCU.

By studying mitochondrial Ca^{2+} uptake induced by a full range of $[Ca^{2+}]_c$, we find that MICU1 knockdown largely activated mitochondrial Ca^{2+} uptake induced by low $[Ca^{2+}]_c$, between 100nM and about 2µM. Instead, for higher $[Ca^{2+}]_c$, the rate of mitochondrial Ca^{2+} uptake was reduced in the MICU1-silenced cells. Our data show that even a $[Ca^{2+}]$ as low as 100nM triggers a fast increase in $[Ca^{2+}]_M$ in MICU1-silenced cells, while it does not produce any effect in the controls. As the $[Ca^{2+}]_c$ is being increased, the rate of mitochondrial Ca^{2+} uptake rapidly increases in the controls so that above 2µM $[Ca^{2+}]_c$, the $[Ca^{2+}]_M$ increase gets already larger in the controls than in the MICU1-silenced cells. However, for $[Ca^{2+}]_c$ between 2 and 5µM, it is still apparent that the initial rate of mitochondrial Ca^{2+} uptake is much faster and starts earlier in the MICU1-silenced cells than in the controls. Therefore, our data suggest that removal of the MICU1-block of the MCU channel is a time-consuming step required to open MCU. At $[Ca^{2+}]_c$ above 5µM, the difference in the initial rate of mitochondrial Ca^{2+} uptake is no longer seen, indicating that the rate of removal of the MICU1-block of MCU is much faster at high $[Ca^{2+}]_c$.

We have found another unexpected use-dependent regulation of MCU activity, which is particularly revealed in the MICU1-silenced cells. We find that prolonged opening of MCU by submicromolar $[Ca^{2+}]$ in these cells triggers an inactivation of the mitochondrial Ca^{2+} entry mechanism activated by MICU1-knockdown. Opening of MCU for 5 min was required for the full inactivation, and half effects were obtained after about 2 min of MCU activation. In addition, once the inactivation has occurred, even prolonged incubation in Ca^{2+}-free medium for up to 15 min was unable to reactivate it. Therefore, in the absence of MICU1, when MCU remains open for several minutes with submicromolar $[Ca^{2+}]_c$, a new block appears that restores the impermeability of MCU at low $[Ca^{2+}]_c$. This mechanism may represent a safeguard against mitochondrial Ca^{2+} overload during prolonged increases in $[Ca^{2+}]_c$. The fact that the inactivation requires such a long time to develop suggests that Ca^{2+} has to enter mitochondria and trigger it from inside. Also, although the inactivation mainly affects Ca^{2+} entry at low $[Ca^{2+}]_c$, a smaller effect can be also observed at higher $[Ca^{2+}]_c$. Thus, prolonged opening of MCU induces a long-lasting MICU1-independent block of MCU, particularly at low $[Ca^{2+}]_c$.

This inactivation mechanism recalls some features of the so called rapid mode of Ca^{2+} uptake into mitochondria (RaM) [15]. However, some other characteristics are different, namely the similar sensitivity to ruthenium red of Ca^{2+} uptake induced by low and high $[Ca^{2+}]_c$, the longer times required for inactivation and the apparent lack of reactivation. Regarding the mechanism of the Ca^{2+}-dependent inhibition, we find it is still present in the absence of ATP and in the presence of several antioxidants. These findings suggest that phosphorylation and reactive oxygen species are probably not involved in the process. Changes in matrix Ca^{2+} buffering resulting from Ca^{2+}-dependent alkalinisation [9] can also be excluded, because similar $[Ca^{2+}]_M$ increases in control cells did not induce any inhibition. The actual mechanism is therefore still unclear.

In conclusion, opening of MCU requires removal of the MICU1-block in a time-consuming step, and the rate of this step is proportional to the $[Ca^{2+}]_c$. This means that the relative amount of MICU1 expression in a particular tissue may control how mitochondria in different cells respond to fast $[Ca^{2+}]_c$ oscillations of low amplitude. Thus, reduced expression of MICU1 would facilitate a more efficient translation to mitochondria of fast and small $[Ca^{2+}]_c$ oscillations. In addition, in the absence of MICU1, prolonged activation of MCU at low $[Ca^{2+}]_c$ leads to an inactivation of the channel response to the same range of low $[Ca^{2+}]_c$. This use-dependent inactivation of MCU may help mitochondria to avoid Ca^{2+} overload during prolonged increases in $[Ca^{2+}]_c$.

AUTHOR CONTRIBUTION

Sergio de la Fuente and Jessica Matesanz-Isabel were responsible for most of the experimental work. Rosalba Fonteriz and Mayte Montero provided additional expertise and laboratory help with most of the experiments. Javier Alvarez directed all of the studies and was primarily responsible for final preparation of the paper before submission, with the assistance of the rest of the team members.

ACKNOWLEDGEMENTS

We thank Pilar Alvarez for excellent technical assistance.

FUNDING

This work was supported by grants from the spanish Ministerio de Ciencia e Innovación (BFU2011-25763) and Junta de Castilla y León (VA029A12-1). Sergio de la Fuente and Jessica Matesanz-Isabel hold FPI (Formación de Personal Investigador) fellowships from the Spanish Government.

REFERENCES

1. Patron, M., Raffaello, A., Granatiero, V., Tosatto, A., Merli, G., De Stefani, D., Wright, L., Pallafacchina, G., Terrin, A., Mammucari, C. and Rizzuto, R. (2013) The mitochondrial calcium uniporter (MCU): molecular identity and physiological roles. J. Biol. Chem. **288**, 10750-10758
2. Perocchi, F., Gohil, V.M., Girgis, H.S., Bao, X.R., McCombs, J.E., Palmer, A.E. and Mootha, V.K. (2010) MICU1 encodes a mitochondrial EF hand protein required for Ca^{2+} uptake. Nature **467**, 291-296
3. De Stefani, D., Raffaello, A., Teardo, E., Szabò, I. and Rizzuto, R. (2011) A forty-kilodalton protein of the inner membrane is the mitochondrial calcium uniporter. Nature **476**, 336-340
4. Baughman, J.M., Perocchi, F., Girgis, H.S., Plovanich, M., Belcher-Timme, C.A., Sancak, Y., Bao, X.R., Strittmatter, L., Goldberger, O., Bogorad, R.L., Koteliansky, V. and Mootha, V.K. (2011) Integrative genomics identifies MCU as an essential component of the mitochondrial calcium uniporter. Nature **476**, 341-345

5. Chaudhuri, D., Sancak, Y., Mootha, V.K. and Clapham, D.E. (2013) MCU encodes the pore conducting mitochondrial calcium currents. Elife **2**, e00704
6. Mallilankaraman, K., Cárdenas, C., Doonan, P.J., Chandramoorthy, H.C., Irrinki, K.M., Golenár, T., Csordás, G., Madireddi, P., Yang, J., Müller, M., Miller, R., Kolesar, J.E., Molgó, J., Kaufman, B., Hajnóczky, G., Foskett, J.K. and Madesh, M. (2012) MCUR1 is an essential component of mitochondrial Ca2+ uptake that regulates cellular metabolism. Nat. Cell Biol. **14**, 1336-1343
7. Plovanich, M., Bogorad, R.L., Sancak, Y., Kamer, K.J., Strittmatter, L., Li, A.A., Girgis, H.S., Kuchimanchi, S., De Groot, J., Speciner, L., Taneja, N., Oshea, J., Koteliansky, V. and Mootha, V.K. (2013) MICU2, a paralog of MICU1, resides within the mitochondrial uniporter complex to regulate calcium handling. PLoS One **8**:e55785
8. Mallilankaraman, K., Doonan, P., Cárdenas, C., Chandramoorthy, H.C., Müller, M., Miller, R., Hoffman, N.E., Gandhirajan, R.K., Molgó, J., Birnbaum, M.J., Rothberg, B.S., Mak, D.O., Foskett, J.K. and Madesh, M. (2012) MICU1 is an essential gatekeeper for MCU-mediated mitochondrial Ca^{2+} uptake that regulates cell survival. Cell **151**, 630-644
9. Csordás, G., Golenár, T., Seifert, E.L., Kamer, K.J., Sancak, Y., Perocchi, F., Moffat, C., Weaver, D., de la Fuente, S., Bogorad, R., Koteliansky, V., Adijanto, J., Mootha, V.K. and Hajnóczky, G. (2013) MICU1 Controls Both the Threshold and Cooperative Activation of the Mitochondrial Ca^{2+} Uniporter. Cell Metab. **17**, 976-987
10. Montero, M., Brini, M., Marsault, R., Alvarez, J., Sitia, R., Pozzan, T. and Rizzuto, R. (1995) Monitoring dynamic changes in free Ca^{2+} concentration in the endoplasmic reticulum of intact cells. EMBO Journal **14**, 5467-5475
11. de la Fuente, S., Fonteriz, R.I., de la Cruz, P.J., Montero, M. and Alvarez, J. (2012) Mitochondrial free [Ca^{2+}] dynamics measured with a novel low-Ca^{2+} affinity aequorin probe. Biochem. J. **445**, 371-376
12. Brini, M., Marsault, R., Bastianutto, C., Alvarez, J., Pozzan, T. and Rizzuto, R. (1995) Transfected aequorin in the measurement of cytosolic Ca^{2+} concentration ($[Ca^{2+}]_c$). A critical evaluation. J. Biol. Chem. **270**, 9896-9903
13. Montero, M., Lobatón, C.D., Moreno, A. and Alvarez, J. (2002) A novel regulatory mechanism of the mitochondrial Ca^{2+} uniporter revealed by the p38 mitogen-activated protein kinase inhibitor SB202190. FASEB J. **16**, 1955-1957
14. Bick, A.G., Calvo, S.E. and Mootha, V.K. (2012) Evolutionary diversity of the mitochondrial calcium uniporter. Science **336**, 886
15. Buntinas, L., Gunter, K.K., Sparagna, G.C. and Gunter, T.E. (2001) The rapid mode of calcium uptake into heart mitochondria (RaM): comparison to RaM in liver mitochondria. Biochim. Biophys. Acta **1504**, 248-261

FIGURE LEGENDS

FIGURE 1. Effect of MICU1 knockdown on the mitochondrial [Ca^{2+}] peak induced by different concentrations of histamine. Panels a-d show the $[Ca^{2+}]_M$ peaks induced by different histamine concentrations in HeLa cells transiently transfected with either MICU1-shRNA (sh) or scrambled shRNA (sc). Data shown are means of 3 different experiments in each case. Panel e shows the statistics of the height of the peaks (mean±s.e., n=3). Panel f shows the silencing obtained in the cell clone expressing the specific MICU1-shRNA compared with the cell clone expressing the scrambled one. Statistics shows the mean±s.e. of 12 determinations. *, $p<0.05$; **, $p<0.01$; ***, $p < 0.001$.

FIGURE 2. Effect of MICU1 knockdown on the rate of mitochondrial Ca^{2+} uptake in permeabilized cells in the presence of different [Ca^{2+}]. HeLa cells transiently transfected with either MICU1-shRNA (sh) or scrambled shRNA (sc) were permeabilized and perfused with different [Ca^{2+}] buffers, as indicated. Single mutated aequorin was used in the experiments of panels a-f. High aequorin consumption precluded longer measurements in panel f. Double mutated aequorin was used in the experiments of panels g and h. Data shown are means of 3 different experiments in each case.

FIGURE 3. Effect of MICU1 knockdown on mitochondrial Ca^{2+} uptake. Panel a shows the dependence of the rate of $[Ca^{2+}]_M$ increase on the cytosolic $[Ca^{2+}]$, obtained from the data of Fig. 2. Panel b shows the changes in the delay of the start of $[Ca^{2+}]_M$ uptake induced by MICU1 silencing, calculated also from the experiments of Fig. 2. Times are measured from the opening of the perfusion electrovalve and include the time required for the arrival of the solution to the cells. *, $p<0.05$. Panel c shows that the increase of $[Ca^{2+}]_M$ induced by 100nM cytosolic $[Ca^{2+}]$ was transient and returned close to resting levels after 10-15 min. Data are mean of 6 different experiments. Panel d shows that the Ca^{2+}-dependent inhibition remained intact when ATP was absent from the perfusion medium. Cells were perfused with ATP-lacking medium for 5 min before and during the addition of Ca^{2+}. Data are mean of 3 different experiments.

FIGURE 4. Effects of FCCP, ruthenium red, Ru360 and MCU silencing on mitochondrial Ca^{2+} uptake in both scramble (sc) and MICU1-silenced (sh) cells. HeLa cells transiently transfected with either MICU1-shRNA (sh) or scrambled shRNA (sc) were permeabilized and perfused with either 10μM $[Ca^{2+}]$ (left panels, using double mutated aequorin) or 1.5μM $[Ca^{2+}]$ (right panels, using mutated aequorin), as indicated, and both in the absence and in the presence of either 2μM FCCP (panels a and b), 4μM ruthenium red (panels c and d) and 500nM Ru360 (panels e and f), added 2 min before the $[Ca^{2+}]$ buffer. In panels g and h, a cell clone with silenced MCU (MCU-) was used for transfection of the scrambled or the MICU1 silencing shRNA, and compared with control HeLa cells. Data shown are means of 3 different experiments in each case.

FIGURE 5. Ca^{2+}-dependent auto-inhibition of the mitochondrial Ca^{2+} uptake activated by MICU1 knockdown. HeLa cells transiently transfected with either MICU1-shRNA (right panels) or scrambled shRNA (left panels) were permeabilized and perfused with 1.5μM $[Ca^{2+}]$ either alone or after previous 5 min perfusion of a $[Ca^{2+}]$ buffer containing either 100nM, 200nM or 500nM $[Ca^{2+}]$. Panel i shows the statistics of the initial rate of mitochondrial Ca^{2+} uptake induced by the addition of the 1.5μM $[Ca^{2+}]$ buffer, either alone (no previous Ca^{2+}) or after previous perfusion of 100, 200 or 500nM $[Ca^{2+}]$. *, $p<0.05$; **, $p<0.01$; ***, $p < 0.005$. Data shown are means of 3 different experiments in each case.

FIGURE 6. Time course of the auto-inhibition of the mitochondrial Ca^{2+} uptake activated by MICU1 knockdown. Panels a-e. HeLa cells transiently transfected with MICU1-shRNA were permeabilized and subjected to two consecutive stimulations with a 500nM $[Ca^{2+}]$ buffer, with an interval of 5 min between them. The second $[Ca^{2+}]_M$ increase was progressively restored when the duration of the first stimulus was reduced from 5min to 15s. Panel f shows the statistics of this effect (n=3; *, $p<0.05$; **, $p<0.01$; ***, $p < 0.001$). Panel g shows the effect in the same cells of the perfusion of the 500nM $[Ca^{2+}]$ buffer on a subsequent addition of a 3.5μM $[Ca^{2+}]$ buffer (statistics on the inset, n=3). Panel h shows that the 500nM $[Ca^{2+}]$ buffer did not produce any change in the mitochondrial membrane potential measured with TMRE. The traces shown are the mean of 14 (scRNA) and 37 (shRNA) cells present in the microscope field, and are representative of 7 similar experiments of each type. Panels i and j show that the 500nM $[Ca^{2+}]$ buffer produced little effects on a second addition of either 500nM or 3.5μM $[Ca^{2+}]$ in cells transfected with scrambled shRNA (statistics on the inset, n=3). $[Ca^{2+}]$ data shown are means of 3 different experiments in each case.

Biochemical Journal Immediate Publication. Published on 09 Dec 2013 as manuscript BJ20131025

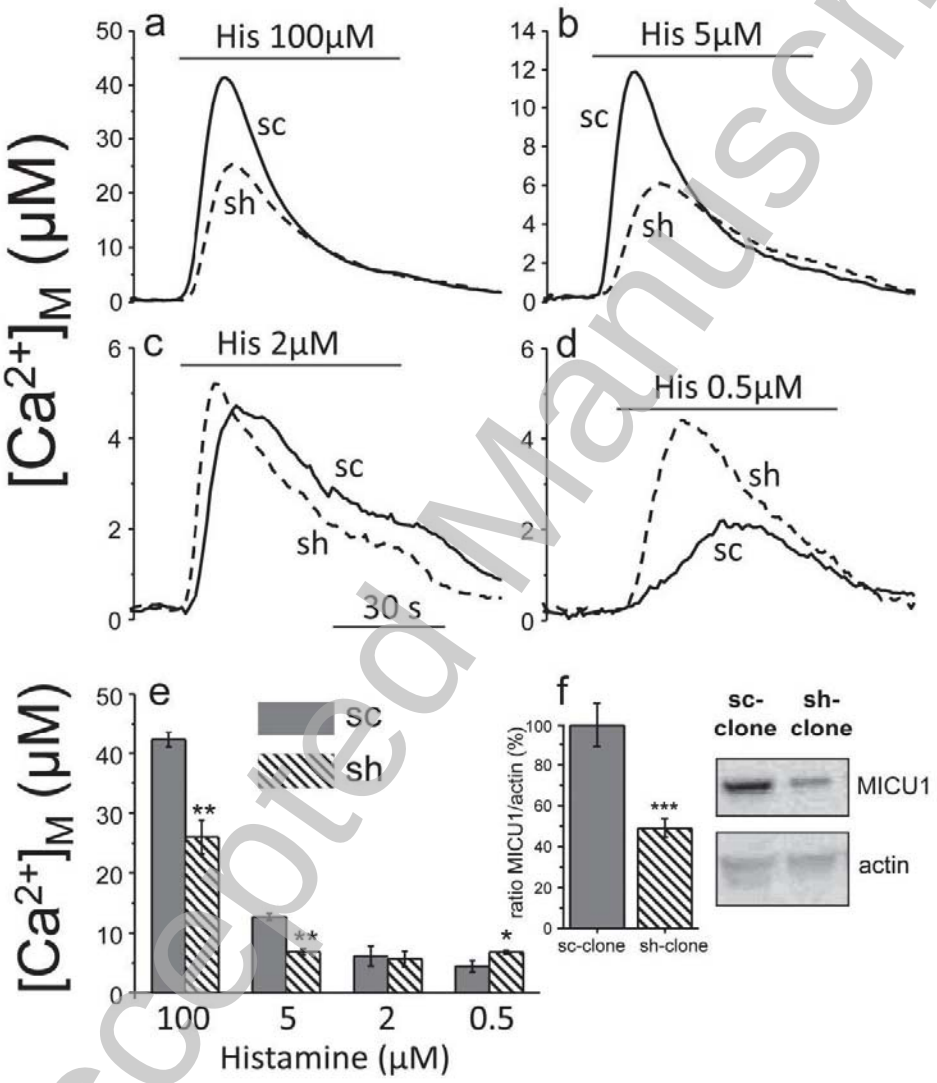

Fig. 1

Biochemical Journal Immediate Publication. Published on 09 Dec 2013 as manuscript BJ20131025

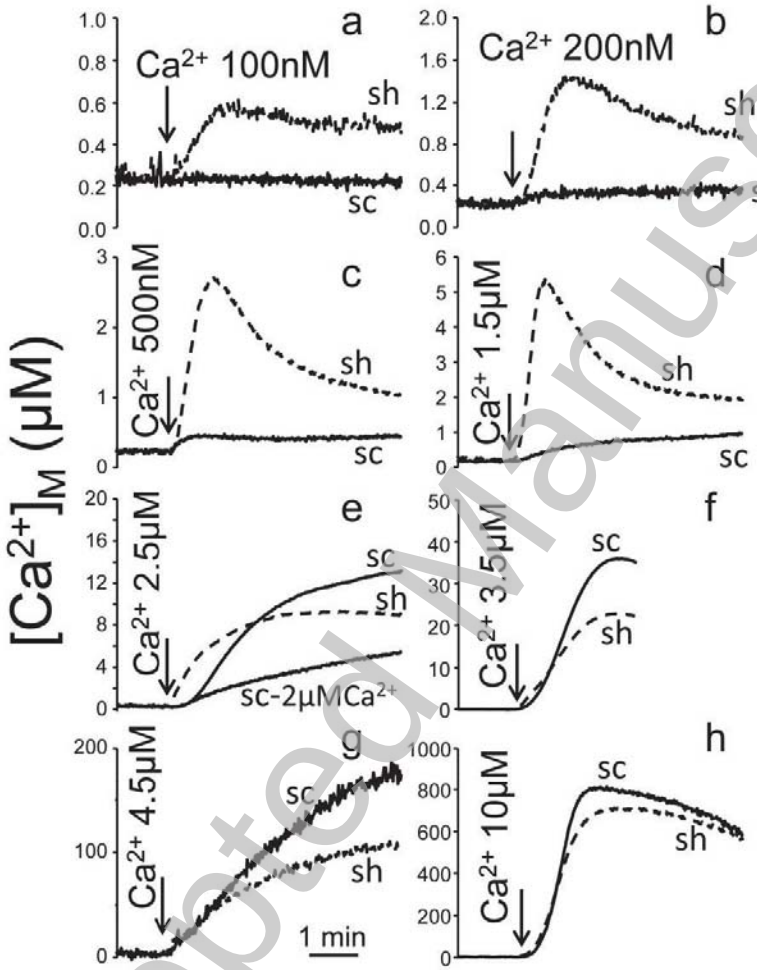

12

Fig. 2

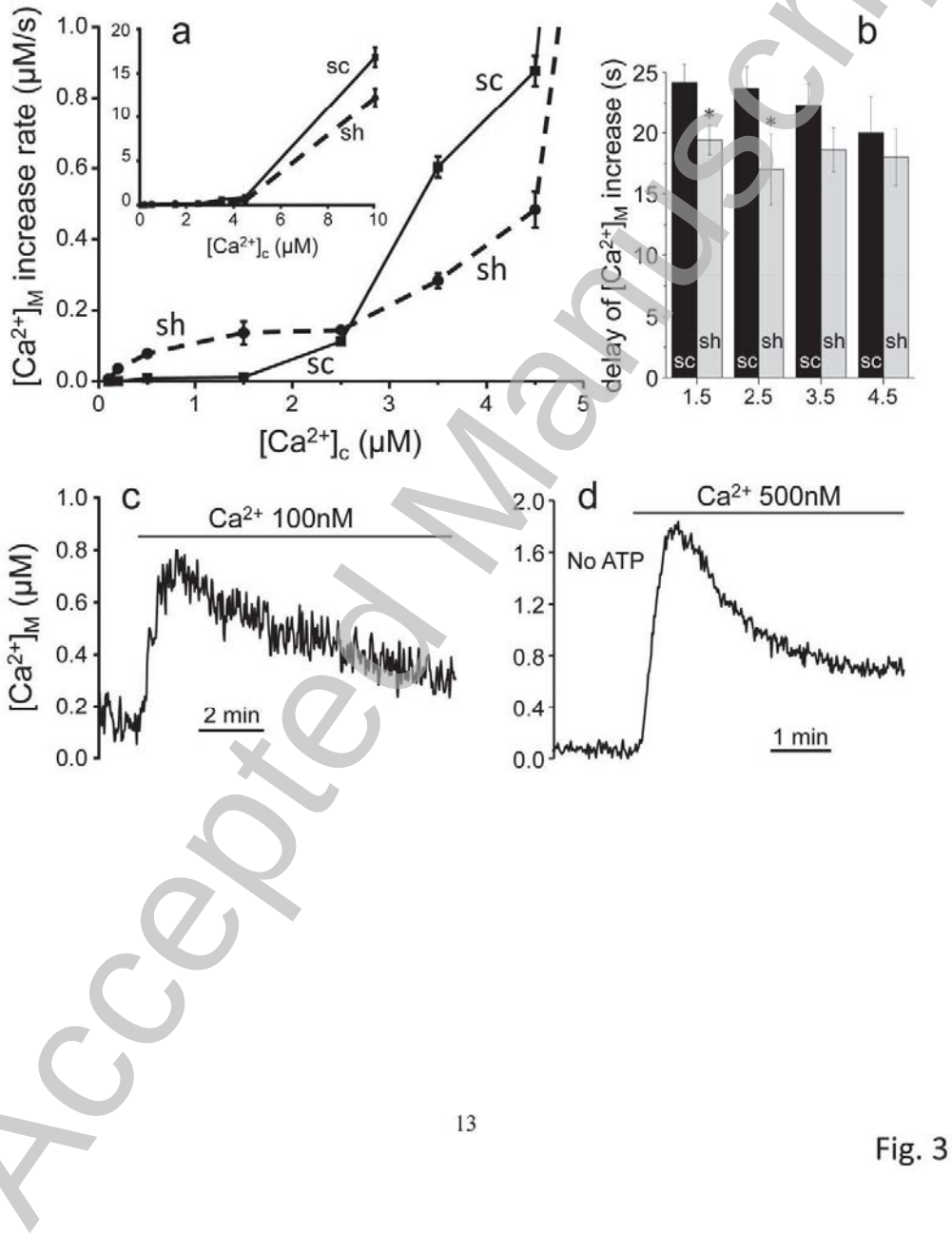

Fig. 3

Biochemical Journal Immediate Publication. Published on 09 Dec 2013 as manuscript BJ20131025

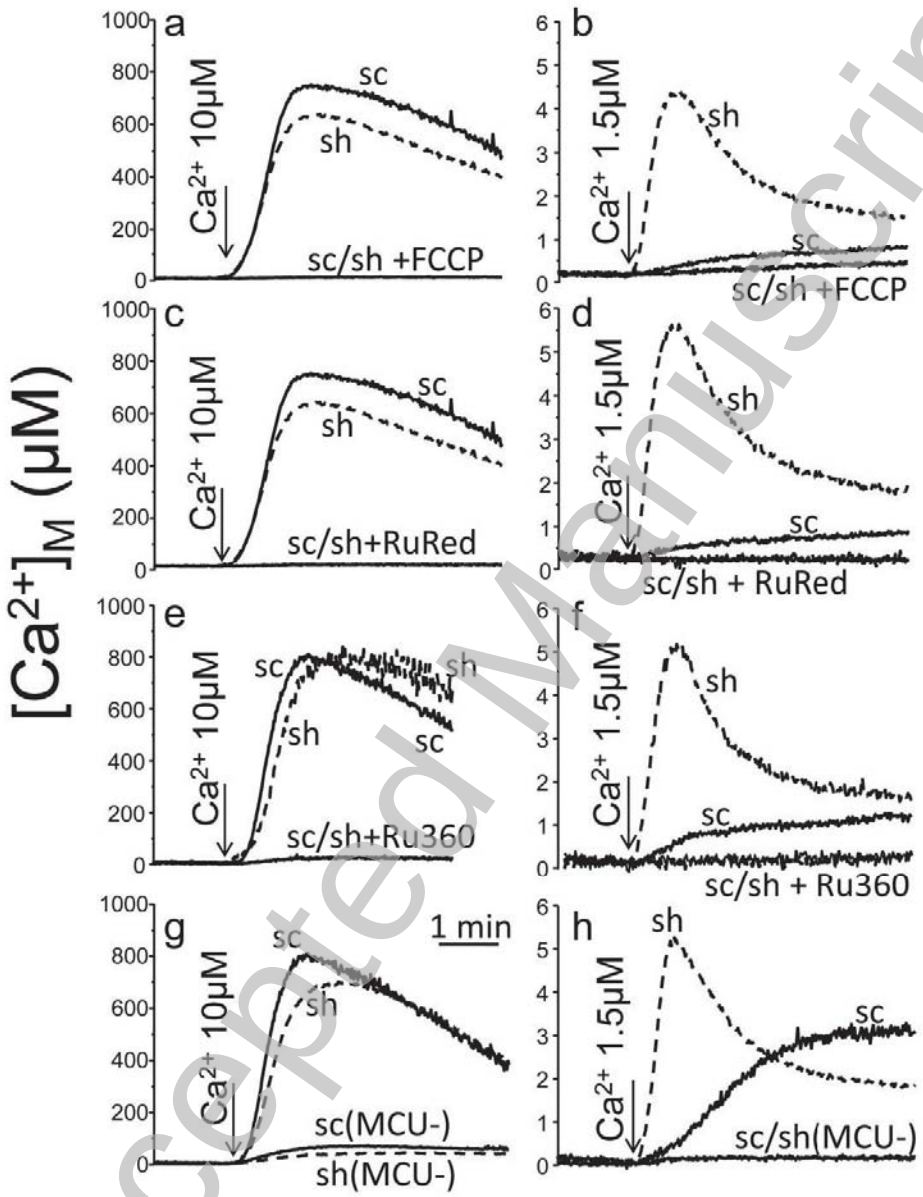

Fig. 4

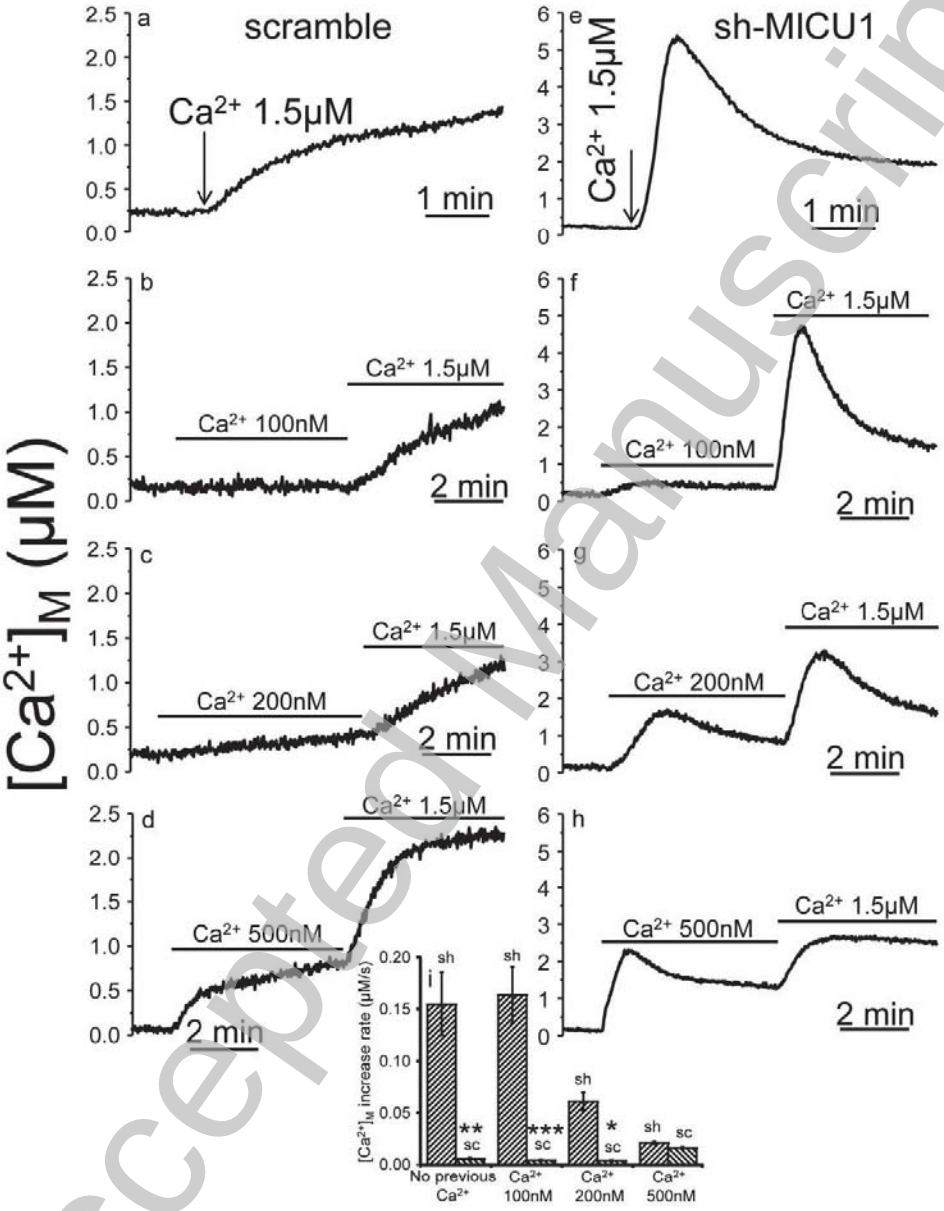

Fig. 5

Biochemical Journal Immediate Publication. Published on 09 Dec 2013 as manuscript BJ20131025

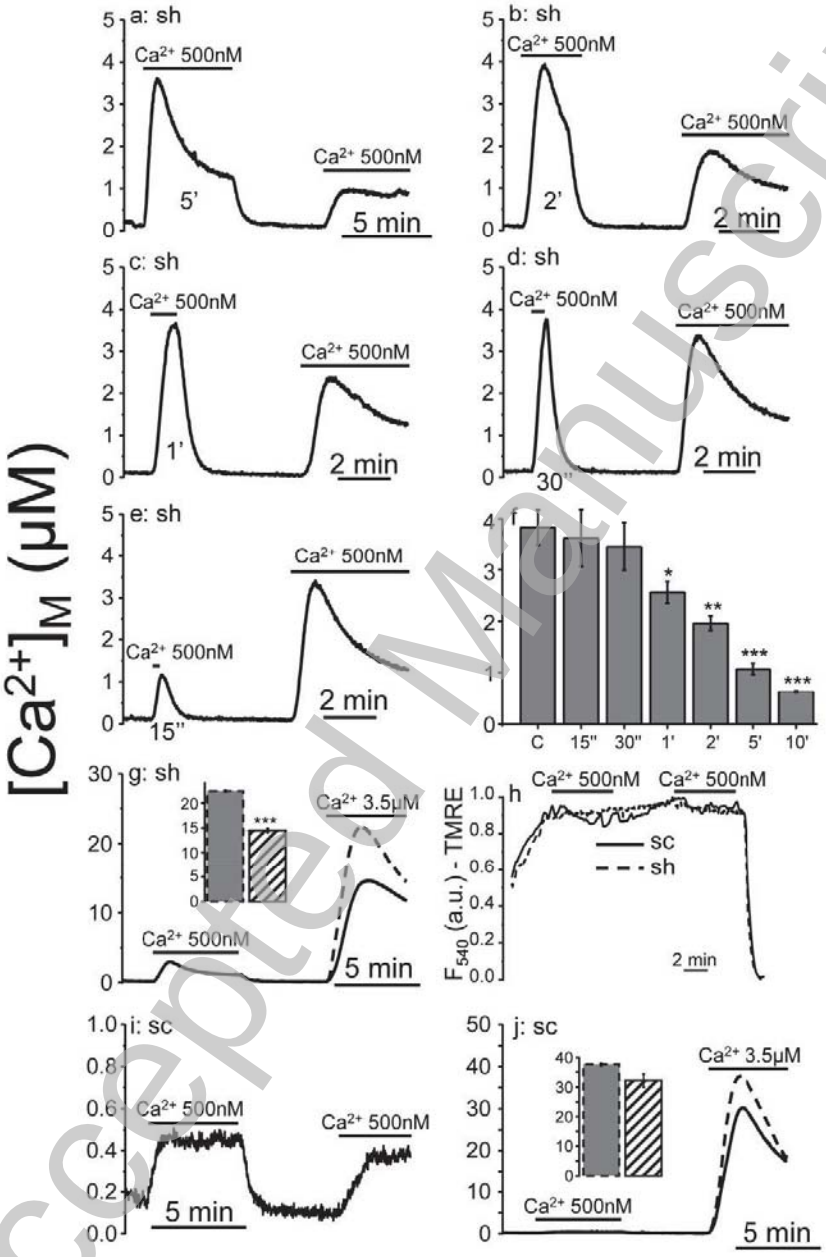

Fig. 6